

Yueqiang Liu, S. Saarelma, M.P. Gryaznevich, T.C. Hender, D.F. Howell  
and JET EFDA contributors

# Modelling Resonant Field Amplification Due to Low-n Peeling Modes in JET

“This document is intended for publication in the open literature. It is made available on the understanding that it may not be further circulated and extracts or references may not be published prior to publication of the original when applicable, or without the consent of the Publications Officer, EFDA, Culham Science Centre, Abingdon, Oxon, OX14 3DB, UK.”

“Enquiries about Copyright and reproduction should be addressed to the Publications Officer, EFDA, Culham Science Centre, Abingdon, Oxon, OX14 3DB, UK.”

The contents of this preprint and all other JET EFDA Preprints and Conference Papers are available to view online free at [www.iop.org/Jet](http://www.iop.org/Jet). This site has full search facilities and e-mail alert options. The diagrams contained within the PDFs on this site are hyperlinked from the year 1996 onwards.

# Modelling Resonant Field Amplification Due to Low-n Peeling Modes in JET

Yueqiang Liu, S. Saarelma, M.P. Gryaznevich, T.C. Hender, D.F. Howell  
and JET EFDA contributors\*

*JET-EFDA, Culham Science Centre, OX14 3DB, Abingdon, UK*

*EURATOM-UKAEA Fusion Association, Culham Science Centre, OX14 3DB, Abingdon, OXON, UK*

*\* See annex of F. Romanelli et al, "Overview of JET Results",  
(Proc. 22<sup>nd</sup> IAEA Fusion Energy Conference, Geneva, Switzerland (2008)).*



## ABSTRACT.

The MHD code MARS-F is used to model low- $n$ , low frequency, large amplitude Resonant Field Amplification (RFA) peaks observed in JET low pressure plasmas. The resonant response of a marginally stable,  $n = 1$  ideal peeling mode is offered as a candidate to explain the experimental observation. These RFA peaks can potentially be used as an active MHD spectroscopy tool to predict the stability of the Edge Localised Mode (ELM).

## 1. INTRODUCTION

It is well known that plasmas in various fusion devices are capable of amplifying externally applied or error magnetic fields, due to the resonant response of metastable modes in the plasma to these fields. This phenomenon is called Resonant Field Amplification (RFA) [1]. Normally, we are concerned about RFA induced by low- $n$ , low frequency fields. One such example is the RFA caused by the Resistive Wall Mode (RWM), either intrinsically stable at low plasma pressures, or marginally stabilised by the plasma rotation or kinetic effects at high pressures. This type of RFA has been extensively studied during recent years in both experiments [2, 3, 4, 5, 6, 7, 8, 9, 10, 11, 12] and in theory [13, 14, 15, 16, 10, 17].

The low-frequency/static RFA due to other stable MHD modes is less investigated, partially due to the fact that many MHD modes (Alfvén eigenmodes, internal kink, infernal mode, tearing modes, ballooning modes, etc.) either have high rotation frequency, or high  $n$  numbers, such that they cannot be in resonance with low- $n$ , low frequency external fields.

There is, however, recent experimental evidence in JET showing the plasma RFA response by other modes than the resistive wall mode. In these JET discharges at low plasma pressures, large, almost static,  $n = 1$  magnetic signals are systematically picked up by the RFA sensor coils. These sensor coils, located at the outboard mid-plane just outside the JET vacuum vessel, detect the radial flux at a toroidal angle, 90 degrees shifted with respect to the Error Field Correction Coils (EFCC) currents. This radial flux, normalised by the direct vacuum field pickup at 0 degree toroidal phase shift, is defined as the RFA response in JET. These pick-up signals measure the pure plasma response field (i.e. without the vacuum field produced by the EFCC currents).

Figure 1 shows two examples, where a standing wave  $n = 1$  external field is launched at 20Hz by the EFCCs in two similar JET Pulse No's: 70199 and 70200. Two peaks of the measured RFA amplitude occur at  $\beta_N$  about 2.3 and 2.0, respectively, which are below the estimated no-wall beta limits (about 2.9 and 2.5 respectively). It is unlikely that these two peaks contain a dominant contribution from the response of a stable RWM. Besides, experimental evidence suggests a correlation between these low frequency RFA signals and the Edge Localised Mode (ELM) free period prior to the first ELM [18]. The objective of this work is to explain these RFA peaks.

In the next Section, using the MHD code MARS-F [19], we compute the RFA response of the marginally stable  $n = 1$  peeling mode, that gives a response amplitude matching reasonably well the experimental data.

## 2. RFA DUE TO STABLE PEELING MODES

For the peeling mode modelling, we use an equilibrium, reconstructed at one time slice from the JET Pulse No: 70200. We emphasise that our objective is not to model the whole time history of the RFA response as shown in Fig.1, during which the plasma equilibrium is evolving. We aim only at explaining the RFA peaks shown in these JET pulses. For instance, the detailed reason of the RFA drop after the peaks, associated with the onset of the first ELM [18] and probably related to the modification of the pedestal current and pressure profiles, is out of the scope of this study.

Figure 2 shows the equilibrium profiles. Note that a finite current density is artificially maintained and adjusted near the plasma edge, in order to obtain unstable/stable peeling modes, which are driven by the edge current density [20]. No experimental constraint, except fixing the total plasma current, is applied in adjusting the edge current density. Using the profiles shown in Fig.2, we generate a series of equilibria, by scaling the amplitude of the plasma pressure, while freezing the current and pressure profiles, as well as keeping the total plasma current at 1.19MA and the on-axis vacuum toroidal field at 1.88T. This procedure leads to a variation of the edge  $q$  value around an integer number with increasing  $\beta_N$ , as shown by Fig.3. For the case considered here, at low plasma pressures  $\beta_N < 0.45$ , the edge  $q$  value falls just below 6, and MARS-F computes an unstable  $n = 1$  peeling mode. At high pressures  $\beta_N > 2.51$ , another unstable domain appears due to the onset of the pressure driven external kink mode (RWM). In between is a region where both the  $n = 1$  peeling and the ideal kink are stable. We compute the  $n = 1$  plasma RFA response in this stable domain. We point out that this  $q_a - \beta_N$  stability diagram (the stability boundary of the peeling mode in terms of  $\beta_N$ ) is very sensitive to the adjustment of the edge current density. Hence the modelling results should not be directly compared with that shown in Fig.1, in terms of the  $\beta_N$  values. This way of generating the equilibria series, though being a general practice in the beta limit study, may not be the best for modelling the peeling mode. Nevertheless, we do obtain a transition of the peeling mode stability at very low  $\beta_N$ . We will also exploit another way of generating the equilibria series later on.

We point out that the edge  $q$  value is generally not defined (infinity) in a diverted plasma. In the simulation, however, we slightly smooth the plasma boundary near the X point to obtain a finite edge  $q$  value. This smoothing procedure does change the peeling mode stability [21]. Fortunately in this study, we are mainly concerned by the RFA response of a marginally stable peeling mode, which can be obtained either by the stabilising effect of the X point [21], or by varying the finite  $q_a$  value. In this simulation, the peeling mode stability is dictated by the  $q_a$  variation, associated with increasing  $\beta_N$ . In experiments, the cause of the peeling mode stability is probably more complicated (X point stabilisation, pedestal bootstrap current variation with  $\beta_N$ , etc.). In order to interpret experiments with the simulation results, the underlying assumption is that the RFA response of a stable, low  $n$  peeling mode is not sensitive to how the mode becomes stable.

Figure 4(a) shows a typical eigenmode structure of an unstable  $n = 1$  peeling mode (at  $q_a = 5.96$ ,  $\beta_N = 0.30$ ), computed for the JET plasma using MARS-F. The radial profiles of the poloidal Fourier harmonics of the plasma displacement are plotted. A straight field line flux coordinate system is

used. For a comparison, the eigenfunction of an unstable  $n = 1$  ideal external kink mode ( $q_a = 6.74$ ,  $\beta_N = 3.62 > \beta_N^{\text{no-wall}} = 2.51$ ) is plotted in Fig. 4(b). We observe two distinguishing features between the peeling and the kink modes: i) the displacement of external kink has a global structure across the whole plasma column, whilst the displacement for the peeling mode is strongly localised towards the plasma edge; ii) the external kink mode has a much richer poloidal spectrum than the peeling mode. The latter, as shown in Fig. 4(a), has a  $m = 6$  dominant poloidal harmonic. This peeling mode structure is retained for all cases that we have examined.

Contrary to the external kink mode, which is strongly suppressed by the presence of a highly conducting wall surrounding the plasma (hence the RWM), the stability of the ideal peeling mode is marginally affected by the wall. Moreover, whilst the RWM is fully stabilised by the rapid plasma rotation in JET, the peeling mode is hardly stabilised by the plasma rotation, as shown by the following two figures.

Figure 5 shows two rotation profiles used in the simulation. These two profiles differ only at the plasma edge, where one vanishes at the plasma boundary (labelled “ROT A”), and the other maintains a finite edge rotation (labelled “ROT B”). Since the peeling mode is localised at the plasma edge, this allows the investigation of how different edge rotation affects the peeling mode response. The rotation profile in the plasma core region represents a typical JET case from the RFA experiments. The core toroidal plasma rotation is normally fast in these JET plasmas, as a result of high momentum input by the neutron beam heating. In our RFA calculations, we assume that the central plasma rotation speed is 3% of the Alfvén speed.

Figure 6 shows the real and imaginary parts of the peeling mode growth rate, in the presence of the JET wall, versus the edge plasma rotation frequency. The rotation profile labelled “ROT B” (Fig.5) is assumed. Three JET equilibria are considered, with  $\beta_N$  values at 0.3, 0.15 and 0, corresponding to the edge  $q$  values at 5.96, 5.92, 5.89, respectively (see Fig. 3). For the rotation speed within the experimental values, the edge plasma rotation introduces a finite mode rotation at the same frequency, without a noticeable modification of the mode growth rate. Note that the induced mode frequency is relatively small, because of a slow rotation at the plasma edge.

The stability of the peeling mode, however, is sensitive to the edge  $q$  values, as shown by Fig.7. On the left side of the figure, we plot the computed growth rate (normalised by the Alfvén time at the plasma centre) of the peeling mode versus  $\Delta \equiv q_a - 6$ . The mode rapidly becomes stable as  $q_a$  approaches an integer number. The mode remains stable as the edge  $q$  value exceeds 6, for a wide range of  $q_a$ . We compute the response (RFA) of this stable branch of the peeling mode to the external field generated by the EFCC currents. The results are plotted on the right side of Fig.7. The RFA amplitude is defined as the ratio of the amplitude of the total flux  $\psi_{\text{tot},r}^0$ , measured at a  $90^\circ$ -shifted toroidal angle with respect to the EFCC current, to the amplitude of the total flux  $\psi_{\text{tot},a}^0$ , measured with a toroidal phase alignment with the EFCC current [22]

$$|\text{RFA}| = \frac{\psi_{\text{tot},r}^0}{\psi_{\text{tot},a}^0}$$

For the EFCC and sensor coil geometry in JET, the total flux  $\psi_{\text{tot},a}^0$  predominantly measures the vacuum field from the EFCC current. The flux  $\psi_{\text{tot},r}^0$  measures the pure plasma response (i.e.  $\psi_{\text{tot},r}^0 = 0$  in vacuum). This RFA definition is used in both experiments and the modelling. An ac standing wave at  $\omega_{\text{ext}} = 1.2 \times 10^{-4} \omega_A$  is used to excite the plasma response. This frequency roughly corresponds to 20Hz used in the experiments. A plasma response, with the amplitude approximately matching that measured in the experiments (see Fig.1), is computed.

The RFA calculations are performed with two different damping models, namely the parallel sound wave damping model, with a numerically adjustable coefficient specifying the damping strength, that mimics the ion Landau damping of sound waves [23], and the drift kinetic damping involving the precessional drift resonances of trapped thermal particles with the mode [24]. The results shown in Fig.7 are obtained by assuming a strong sound wave damping, which seems to describe well the plasma dynamics in high beta tokamaks.

Figure 8 compares the computed RFA amplitude under various assumptions on the damping model and the rotation profile used in the simulation. At  $\Delta$  close to 0, the peeling mode is marginally stable, whilst the RWM is deeply stable because of very low  $\beta_N$ . Therefore, the RFA in this case is dominated by the peeling mode response. Figure 8 shows that the stable peeling mode response is not very sensitive to the plasma rotation profile or to the damping model.

With increasing  $\Delta$ , thus increasing  $\beta_N$  (in the model here), the peeling mode becomes more stable, and the RWM starts to give a dominant contribution to the plasma response. In this case, we observe a sensitive dependence of the RFA on plasma rotation profile and on the damping model. In particular, with the full kinetic damping model, the difference in the edge plasma rotation gives a substantial difference in the computed RFA response near the no-wall beta limit, corresponding to  $\Delta = 0.48$ . [The RFA response due to a stable RWM starts to grow before the plasma pressure reaches the no-wall limit [22].]

In order to separate the contributions from the peeling mode and from the stable RWM, we investigate a series of equilibria, where we keep a constant low pressure  $\beta_N = 1.0$ , and vary slightly the total plasma current (without changing the toroidal magnetic field) to scan  $q_a$ . The equilibrium profiles are also unchanged during the  $q_a$  scan. We expect that the contribution of the stable RWM to the RFA is small at this low  $\beta_N$  value. Figure 9 shows the computed RFA amplitude versus the peeling mode stability parameter  $\Delta$ . The  $n = 1$  peeling mode is stable as  $\Delta$  exceeds 0. Both static and standing wave (with a frequency approximately matching the experimental value) probing currents are assumed. The computed RFA amplitudes largely agree with the experimental measurements shown in Fig.1, with the strongest response occurring at  $\Delta = 0$ , corresponding to a marginally stable peeling mode. The RFA response of the peeling mode is not sensitive to the damping models, in contrast to the RWM, whose stability and response is significantly affected by the mode resonance with plasma particles or waves. We point out that it is difficult to make a direct comparison of the computed RFA with experimental data, due to the fact that, for a given  $\beta_N$ , the value of  $\Delta$ , which controls the stability of the peeling mode, depends on the precise details of the equilibrium, especially the current profile



at the plasma edge. We also mention that the experimental RFA response, measured near the no-wall beta limit for the ideal external kink mode, is dominantly caused by the stable RWM.

## CONCLUSION AND DISCUSSION

The effect of resonant field amplification, due to the response of the low- $n$  MHD modes to the externally applied magnetic fields, is modelled for JET plasmas using the MARS-F code.

Some of the RFA peaking events, observed in JET discharges prior to the first ELM event at lower plasma pressures, may be explained by the presence of stable  $n = 1$  peeling modes, located at the plasma edge. The simulation results indicate that, unlike the resistive wall mode, the peeling mode response is not very sensitive to the plasma rotation, nor to the kinetic effects. Since the peeling mode is so localised that the outer conductors play a minor role, the response of the mode, like the stability of the mode, is not sensitive to the wall geometry. [The total response, including the wall contribution, to ac coil currents, of course depends on the wall geometry.] Since the mode response tends to peak at the marginal stability point, it may be possible to use the RFA measurement in the experiments, to predict the ELM events caused by the onset of these low- $n$  peeling modes. More analysis of the experimental data is needed to confirm this.

The present study does not cover the full RFA evolution observed in the experiments. A direct, quantitative modelling of the experiments would require an accurate reconstruction (especially the edge plasma current density) of a series of equilibria according to the experimental time trace. This work does however offer qualitative insight into how the approach to the  $n = 1$  peeling mode instability can increase the observed RFA.

## ACKNOWLEDGMENTS

Y.Q. Liu acknowledges many fruitful discussions with Dr. C.G. Gimblett from UKAEA Culham and Dr. V.D. Pustovitov from Kurchatov Institute during this work. We also thank the JET TF-M Leader Dr. H.R. Koslowski, and Dr. A.W. Morris from UKAEA Culham for valuable suggestions in improving the manuscript. This work was funded jointly by the United Kingdom Engineering and Physical Sciences Research Council and by the European Communities under the contract of Association between EURATOM and UKAEA. The views and opinions expressed herein do not necessarily reflect those of the European Commission. Work partly conducted within the framework of the European Fusion Development Agreement.

## REFERENCES

- [1]. Boozer A.H. 2001 Physical Review Letters **86** 5059
- [2]. Okabayashi M. et al 2002 Plasma Physics Controlled Fusion **44** B339
- [3]. Garofalo A.M. et al 2003 Physics of Plasmas **10** 4776
- [4]. Strait E.J. et al 2003 Nuclear Fusion **43** 430
- [5]. Reimerdes H. et al 2004 Physical Review Letters **93** 135002

- [6]. Reimerdes H. et al 2005 Nuclear Fusion **45** 368
- [7]. Reimerdes H. et al 2006 Physics of Plasmas **13** 056107
- [8]. Gryaznevich M.P. et al 2003 Bull. American Physics Society **48** RP1.036
- [9]. Hender T.C. et al 2004 Resistivewall mode studies in JET Proc. 20th IAEA Fusion Energy Conf. 2004 (Vilamoura, Portugal, 2004) (Vienna: IAEA) IAEA-CN-116/EX/P2-22 CD-ROM file EX/P2-22
- [10]. Hender T.C. et al 2006 Prediction of Rotational Stabilisation of ResistiveWall Modes in ITER Proc. 21st IAEA Fusion Energy Conf. 2006 (Chengdu, China, 2006) (Vienna: IAEA) IAEA-CN-149/EX/P8-18 CD-ROM file EX/P8-18
- [11]. Gryaznevich M.P. et al 2007 Experimental identification of the beta limit in JET Proc. 34th EPS Conference on Controlled Fusion and Plasma Physics 2007 (Warsaw, 2007) ECA 31A P1-070
- [12]. Gregoratto D. et al 2005 Physical of Plasmas **12** 092510
- [13]. Gimblett C.G. and Hastie R J 2004 Physics of Plasmas **11** 1019
- [14]. Pustovitov V.D. 2004 Plasma Physics Report **30** 187
- [15]. Zheng L. et al 2005 Physics Review Letters **95** 255003
- [16]. Liu Y.Q. 2006 Plasma Physics Controlled Fusion **48** 969

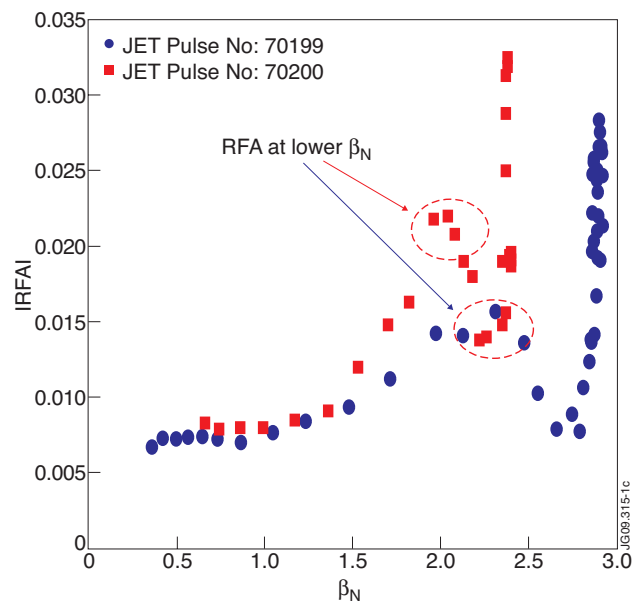


Figure 1: The RFA response measured in the JET Pulse No: 70199.

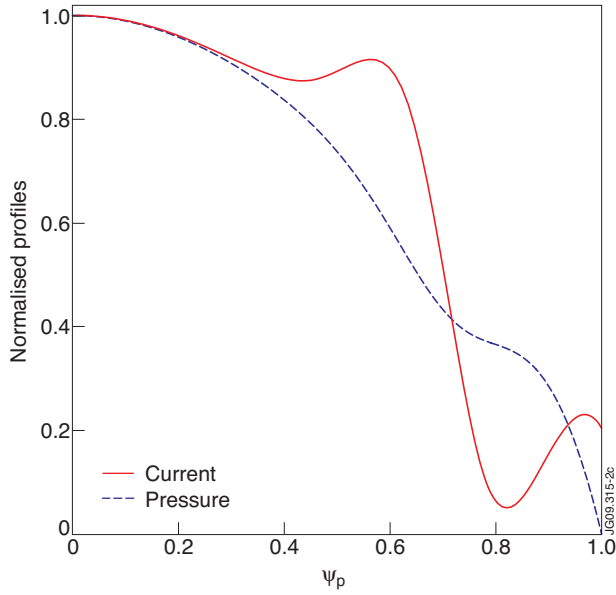


Figure 2: Profiles of the plasma equilibrium current and pressure used in the peeling mode calculations. The equilibrium is re-constructed from a JET Pulse No: 70200. Both profiles are normalised by the corresponding values at the plasma centre.

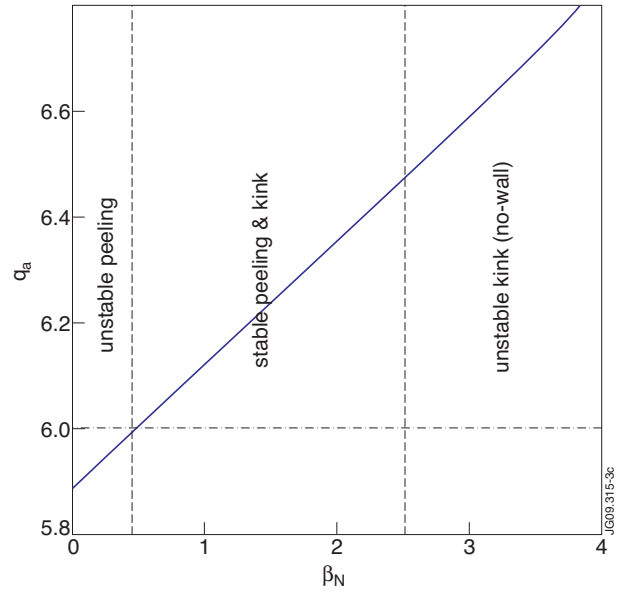


Figure 3: The variation of edge  $q$  value versus the normalised plasma pressure  $\beta_N$ , for a series of the JET equilibria used in the MARS-F simulation. The current profile, as well as the total plasma current, is fixed. The pressure amplitude is scaled without modifying the profile. Two dashed lines indicate the stability boundary for the  $n = 1$  ideal peeling and kink modes respectively.

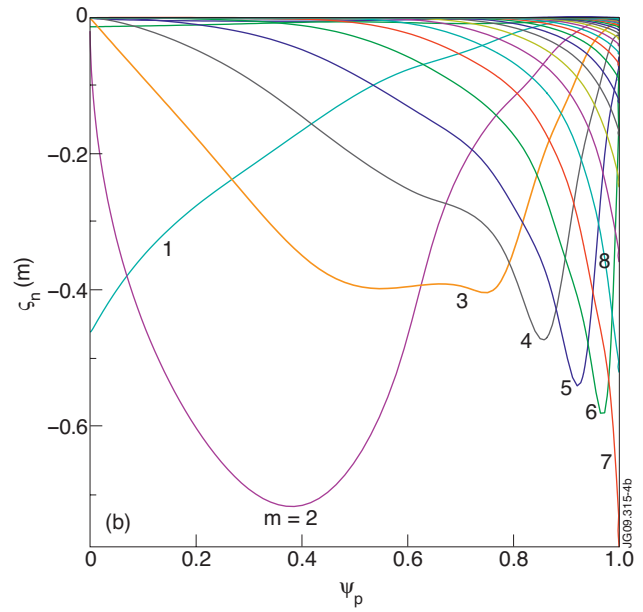
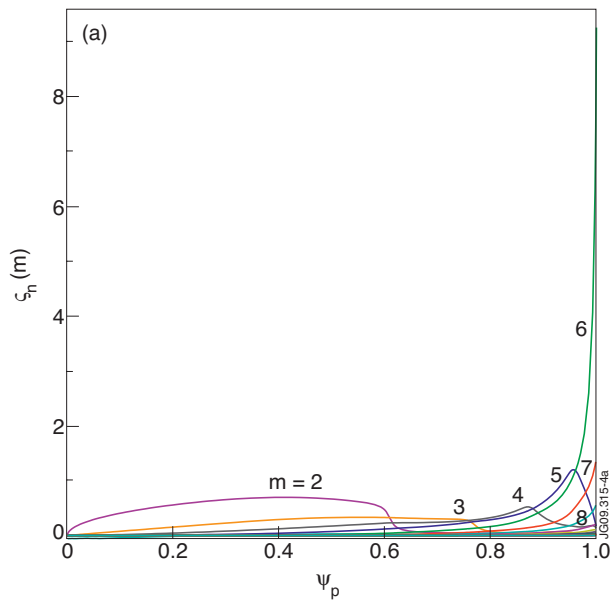


Figure 4: Poloidal Fourier harmonics of the normal displacement in a straight field line coordinate system, computed for (a) the peeling mode, and (b) the external ideal kink mode.

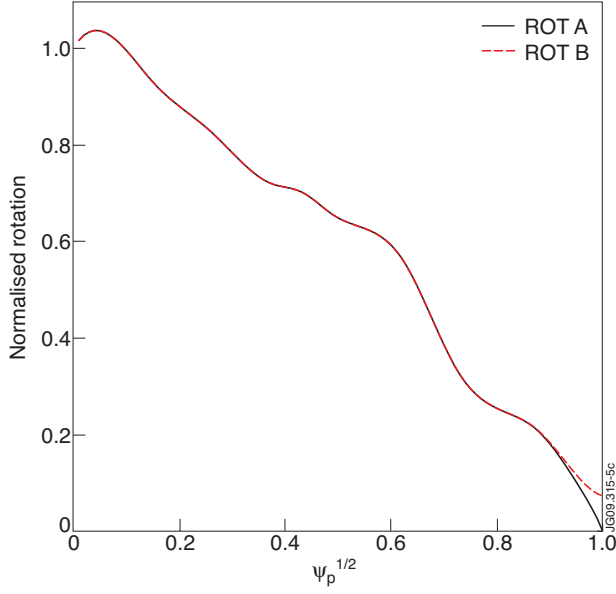


Figure 5: Two plasma rotation profiles considered in the peeling mode modelling. The rotation profile labelled “ROT B” comes from the JET Pulse No: 62024.

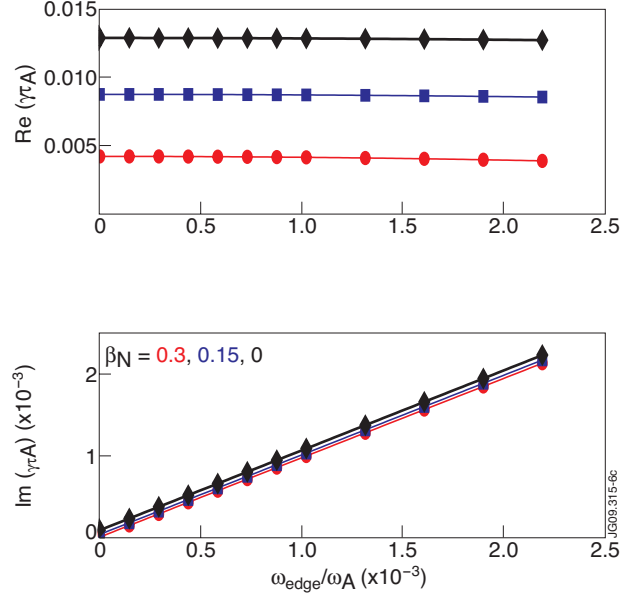


Figure 6: Effect of toroidal edge rotation on the peeling mode stability.

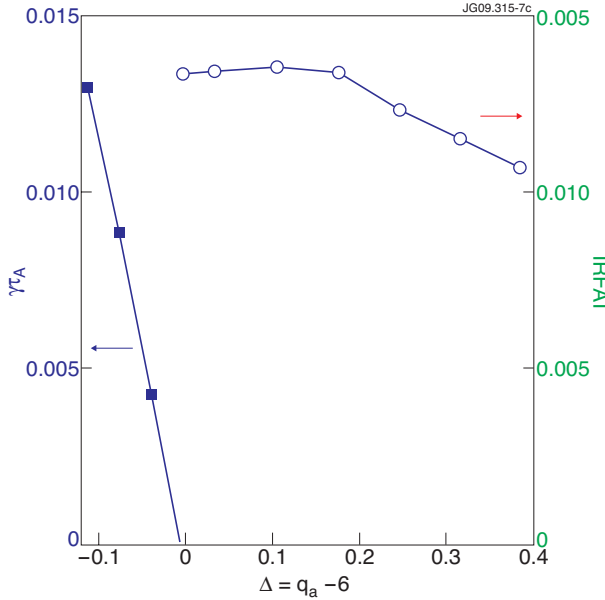


Figure 7: Growth rate of unstable peeling mode, and RFA response of the stable peeling mode, versus the proximity of the edge  $q$  value to an integer number. The rotation profile labelled “ROT A” from Fig.5 is used. A strong parallel sound wave damping model is assumed for the RFA calculations. The ac standing wave excitation at  $\omega_{ext} = 1.2 \times 10^{-4} \omega_A$  is assumed.

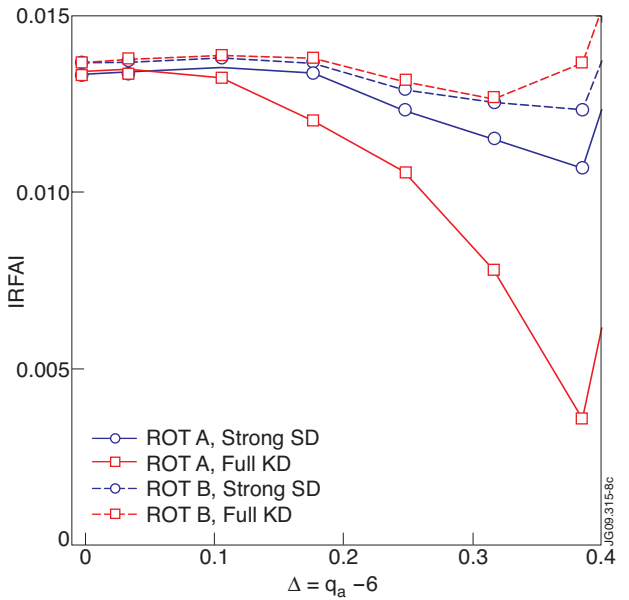


Figure 8: The simulated RFA response of the stable peeling mode, versus the proximity of the edge  $q$  value to an integer number. Two rotation profiles (labelled by “ROT A” and “ROT B” in Fig. 5) are used. A strong parallel Sound wave Damping (SD) model is compared with the full Kinetic Damping (KD) model. The ac standing wave excitation at  $\omega_{ext} = 1.2 \times 10^{-4} \omega_A$  is assumed.

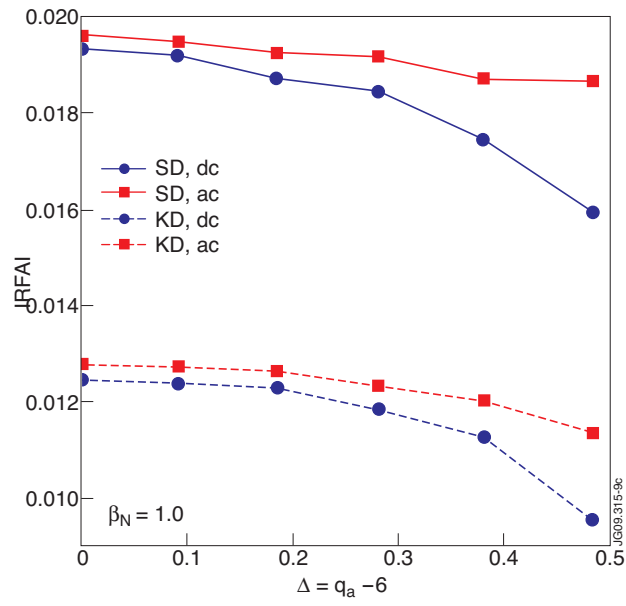


Figure 9. The RFA response of the stable  $n = 1$  peeling mode with different mode damping models (sound wave versus kinetic damping). The dc excitation is compared with an ac standing wave excitation at  $\omega_{ext} = 1.2 \times 10^{-4} \omega_A$ . The rotation profile labelled "ROT A" from Figure 5 is used.